DAMPING, NOISE, AND IN-PLANE RESPONSE OF MEMS ACOUSTIC EMISSION SENSORS

AMELIA P. WRIGHT, WEI WU*, IRVING J. OPPENHEIM and DAVID W. GREVE*
Dept. of Civil & Environmental Engineering, *Dept. of Electrical and Computer Engineering,
Carnegie Mellon University, Pittsburgh, PA 15213

Abstract

Resonant sensors for acoustic emission detection have been designed and fabricated as MEMS capacitive transducers with resonant frequencies between 100 and 500 kHz. We report four recent advances in our understanding of their mechanics and in the implications of those advances for improved sensitivity. One advance involves a successful laboratory method to seal and evacuate the MEMS device within its ceramic package, thereby operating in a coarse vacuum and reducing or eliminating squeeze film and radiation damping effects; we present characterization measurements showing an approximate fourfold increase in quality factor Q. A second advance is a summary of our theoretical analysis of noise sources for a resonant, capacitive MEMS transducer; we report that Brownian noise associated with the impact of air molecules is the major source. A third advance is the use of a grillage of beams, rather than a perforated plate, as the moving plate in the spring-mass system; we present characterization measurements showing a significant reduction in damping and therefore a higher Q. The fourth advance is a finger-type mechanism to sense in-plane motion; we show characterization measurements confirming the resonant behavior of that device and showing that the in-plane device has a much higher Q than comparable out-of-plane devices.

Keywords: Damping; in-plane motion; MEMS; sensor innovation.

Introduction

Our research group has developed a series of MEMS devices to function as resonant transducers sensitive to out-of-plane motion. Their mechanics and their use as acoustic emission sensors are most completely described in a paper by Ozevin *et al.* [1]. The transducers are fabricated in the PolyMUMPS surface micromachining process as spring-mass systems to form capacitors in which the moving plate is an elastic structure in polysilicon with a thickness of 2 μm. We typically place on each chip a suite of transducers at different frequencies in the range up to 500 kHz, placing four transducers on a 5 × 5 mm chip or a larger number of transducers on a 10 × 10 mm chip.

Figure 1a shows a completed four-channel AE sensor system [2, 3]. It consists of a MEMS chip, nominally 5 × 5 mm, containing four independent transducers with resonant frequencies in the range between 126 and 500 kHz. The chip is mounted in a Spectrum Semiconductor Materials CPG06856 pin-grid array ceramic package, 26 × 26 mm, chosen because it provides a smooth bottom surface for coupling to structural plates. The ceramic package engages a bottom PC board and Sullins 2.0 mm connectors engage a bottom PC board containing four amplifier circuits, as shown in Fig. 1a, each with a nominal gain of 100 V/V (40 dB). The whole system (apart from the cable connector) is contained in a volume of 35 × 35 × 30 mm.

Vacuum Sealing of a Perforated Plate Transducer

Among various mechanisms limiting the sensitivity of such transducers, the damping effect of air is very significant. Damping occurs both from acoustic radiation into the air and from squeeze-film damping as air is forced through the gap between the moving plate and stationary plate. The effectiveness of a resonant transducer is related to its sharpness of resonance, or (equivalently) to its dynamic magnification, and is commonly calculated as the quality factor Q. Operation in coarse vacuum would reduce the damping effects and increase Q, and we report a practical laboratory method for sealing and evacuating the chip in its ceramic package.

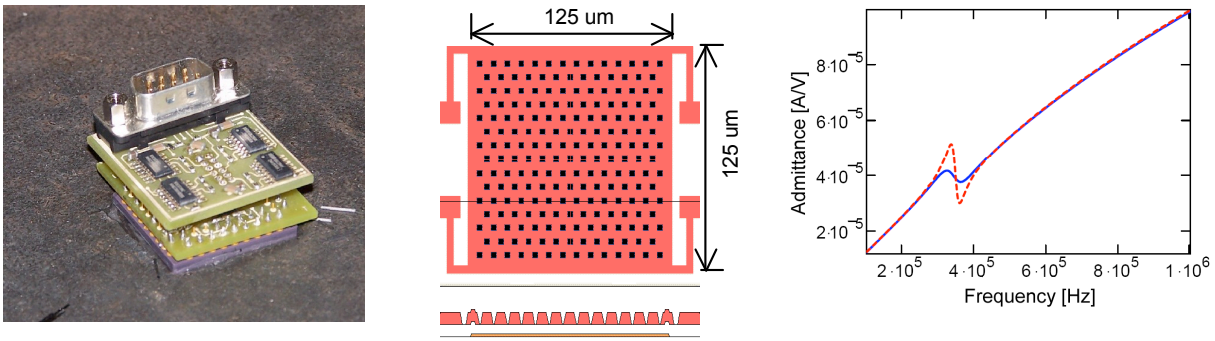

Fig. 1a. Four-channel AE sensor system in 35 × 35 × 30 mm volume.
1b. CAD layout and section of one unit.
1c. Admittance at resonance, f = 443 kHz, Q = 5.5 (atmospheric), Q = 19.7 (evacuated).

Figure 1b is the CAD layout and section of a single unit, showing a perforated square plate (125 µm on a side, with 3.5-µm square etch holes on a triangular grid with 8 µm between holes) suspended by four flexural springs, with a gap of 1.25 µm between the plate and the underlying stationary electrode. FEM simulation was used in selecting the flexural spring length to achieve target design frequencies between 126 and 500 kHz. Each transducer consists of 144 units (a 12 × 12 array) to obtain a target design capacitance near 13 pF. Figure 1c shows the admittance plot for the transducer with nominal design frequency of 500 kHz, and resonance is observed near 443 kHz. The admittance plot shows the sharpness of resonance before and after the process of sealing and evacuation. The broader resonance in Figure 1c is the admittance plot at atmospheric pressure, corresponding to a Q of 5.5.

For the different transducers (different resonant frequencies) the admittance measurements at atmospheric pressure showed Q factors ranging from 1.4 to 5.5, and the measured Q generally increased with transducer frequency, as predicted [1]. In an attempt to make the transducers more sensitive, we next developed a laboratory method to seal and evacuate the device within its package. The CPG06856 ceramic package product has a matching lid, plated with nickel and gold. In our method, a hole is drilled in the solder seal lid, the perimeter of the lid is soldered to the CPG06856 package, and a small amount of solder is dropped around the hole. The package is then moved to a vacuum chamber, within which a soldering iron can translate on a vertical axis. After the chamber is evacuated, the soldering iron is energized and the solder around the hole is melted, sealing the hole in the lid. After the solder cools, the package is removed from the vacuum chamber. This method has proven reliable and the resulting seal appears to be durable.

The sharper resonance in Fig. 1c is an admittance plot repeated 28 days after sealing, showing no loss of vacuum, and corresponding to a Q of 19.7. The increase observed in Q, approximately fourfold, is helpful in increasing the expected sensitivity of the transducer. However, it immediately raises the question, what factor is limiting the Q? The observed Q is substantially lower than that typically observed in polysilicon resonators; for example, other researchers have built resonators in the PolyMUMPS process with a measured Q value between 300 and 550 [4]. It is likely that the observed Q is limited by imperfect coherence in the response of the 144 units that comprise the transducer. The 12×12 array occupies an area less than 2-mm square, which is small compared to the ultrasonic wavelength in steel at the frequencies (below 500 kHz) of our transducers, and therefore it is reasonable to expect that an arriving mechanical excitation will uniformly drive the units in the array. It is more likely that the 144 units do not have identical resonant frequencies. For example, the stiffness of the anchors, assumed to be rigid, will differ from the perimeter of the array to the interior, creating one source for slight deviations in the resonant frequencies. Another likely source of variation in resonant frequencies is variation in the spring constant due to the manufacturing variation in the polysilicon beam width. The effect of imperfect coherence would be a "spreading" of the aggregated peak, which appears as a broader peak in admittance measurements.

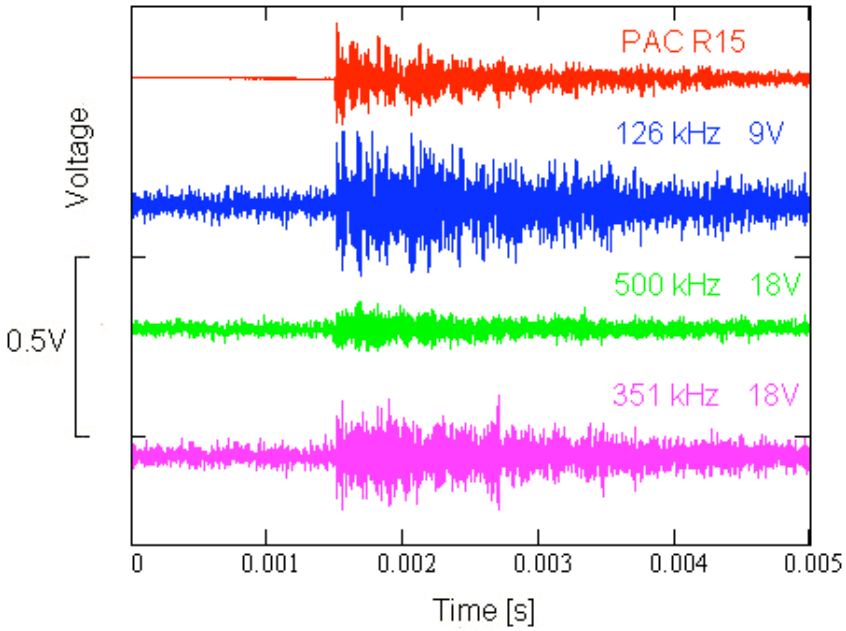

Fig. 2. Pencil lead break response, comparing three MEMS sensors to PAC R15 sensor.

We applied pencil lead breaks on a large steel plate, 9.5 mm thick, with the MEMS system (Figure 1a) and a PAC R15 sensor mounted symmetrically 20 mm from that source. Figure 2 shows the response of three sensor channels on the MEMS device, after onboard amplification, and the raw response of the PAC R15 sensor; for each MEMS channel we indicate in Figure 2 its design frequency and its bias voltage. Signal strength from the sensor channels on the MEMS device is comparable to that from the PAC R15 sensor, although the SNR is not as favorable.

Noise Analysis

We recently developed a theoretical analysis of noise sources in the electromechanical behavior of a resonant, capacitive-type transducer. We examine both Johnson noise from thermal agitation of electrons and Brownian noise from impact excitation of the moving plate by air

molecules. The RMS noise current of Johnson noise is independent of frequency (white noise) and is given by [5]

$$i_{RMS} = G\sqrt{4k_B T\Delta f / R}\,,$$

where G is the amplifier gain, k_B is the Boltzmann constant, T is the absolute temperature, R is the resistance at the amplifier input, and Δf is the bandwidth. We determine that Brownian noise, for example as calculated by Gabrielson [6], is the other mechanism of interest. The spectral density of the squared magnitude of the force [N^2/Hz] caused by air molecules striking a suspended plate with resonant frequency ω_0 is independent of frequency and is given by [6]

$$\left\langle \left|F_B(\omega)\right|^2 \right\rangle = 4k_B T m\omega_0 / Q\,,$$

where m the mass of the diaphragm and $\omega_0 Q$ is the mechanical damping coefficient. The equation of motion for the displacement $x(t)$ of the diaphragm is

$$\ddot{x} + \frac{\omega_0}{Q}\dot{x} + \omega_0^2 x = \frac{F_B(t)}{m}\,,$$

where $F_B(t)$ is the Brownian force. Taking the Fourier transform and solving for the velocity spectral density, $V(\omega)=j\omega X(\omega)$, gives

$$V(\omega) = \frac{F_B(\omega)/m}{j\omega + \dfrac{\omega_0}{Q} + \dfrac{\omega_0^2}{j\omega}}$$

from which we find for the ensemble average

$$\left\langle \left|V(\omega)\right|^2 \right\rangle = \frac{\left\langle \left|F_B(\omega)/m\right|^2 \right\rangle}{\left(\omega - \dfrac{\omega_0^2}{\omega}\right)^2 + \left(\dfrac{\omega_0}{Q}\right)^2}\,.$$

The current in the external circuit is related to velocity spectral density through

$$i(t) = \frac{d(CV_{DC})}{dt} = V_{DC}\frac{dC}{dt} = \frac{V_{DC}C_0}{g}v(t)$$

where V_{DC} is the applied DC bias, g the gap between plates, A the plate area, and $C_0=\varepsilon_0 A/g$ is the capacitance between the plates. Consequently, in the frequency domain

$$\left\langle \left|I(\omega)\right|^2 \right\rangle = (V_{DC}C_0/g)^2 \left\langle \left|V(\omega)\right|^2 \right\rangle$$

and integrating over the amplifier bandwidth we have for the RMS noise current

$$i_{RMS}{}^2 = \frac{1}{2\pi}\left(\frac{V_{DC}C_0}{g}\right)^2 \int_0^{2\omega_H} \frac{4k_B T\omega_0/(mQ)}{\left(\omega - \dfrac{\omega_0^2}{\omega}\right)^2 + \left(\dfrac{\omega_0}{Q}\right)^2} d\omega\,.$$

The argument of the integral captures the dynamic response of the resonator to air molecule impact, and therefore shows a dependence upon the quality factor Q, together with the influence of amplifier bandwidth. However, if the amplifier bandwidth ω_H encloses the resonant peak, during contour integration (not shown) the upper limit of the integral can be extended to infinity. In this case, the result,

$$i_{RMS}^{\ 2} = \left(\frac{V_{DC} C_0}{g} \right)^2 \frac{k_B T}{m},$$

is almost independent of Q. Physically, increasing the resonator Q increases the velocity resulting from a particular collision. However the width of the resonance decreases with Q, resulting in an RMS noise level that is independent of Q. The noise thus consists of a frequency-independent component due to Johnson noise and a peaked component due to Brownian noise.

Table 1 shows the predicted noise voltage at the output of the amplifier for an amplifier gain of 100 V/V and in input resistor of 160 kΩ. The predicted RMS noise voltage is independent of Q. (Our devices have the same area and gap, and the only other parameter leading to a different noise prediction would be the DC bias voltage, which was 9 V for all transducers). Also shown is the measured RMS noise voltage for three transducers with an amplifier of bandwidth 800 kHz. The measured and predicted noise voltages confirm the deduction from the noise analysis, that the RMS noise voltage is independent of Q. This suggests that the performance of the transducer is limited by the combination of Brownian and Johnson noise, rather than amplifier noise and interference.

Table 1. Predicted and measured RMS noise at output of amplifier.

Frequency Measured [kHz]	Q Measured	Brownian Noise Predicted [mV]	Johnson Noise Predicted [mV]	Noise Measured [mV]
126	1.4	12	5	14
351	4.8	12	5	22
500	5.5	12	5	19

Grillage Transducer for Out-of-Plane Motions

We report on a new transducer mechanism, fabricated in 2007, an out-of-plane sensor with a design frequency of 250 kHz. The design features a moving plate constructed as a grillage rather than as a perforated plate with periodically spaced etch holes. We show characterization measurements suggesting two advantages to the grillage geometry. Capacitance measurements and FEM simulations show the grillage to approximate a whole plate in its electrical behavior, and admittance measurements show the grillage to have higher Q (lower damping) than a comparable perforated plate.

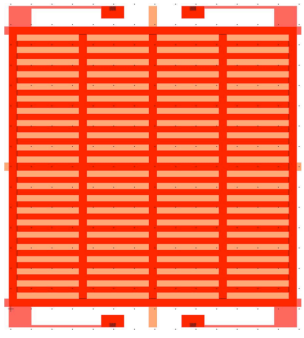

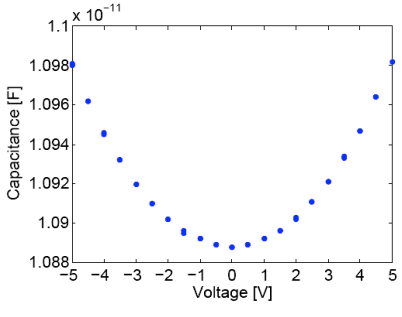

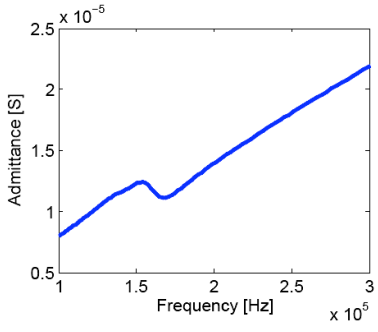

Fig. 3a. CAD layout of grillage unit for out-of-plane sensing.
3b. C-V plot, C_0 = 10.9 pF.
3c. Admittance at resonance, f = 160 kHz, Q = 6.7.

Figure 3a is the CAD layout of a single unit, showing a grillage (outside dimensions 138 × 140 μm) supported by four flexural springs; the beams forming the grillage are 3 μm in width, with a clear spacing of 3 μm between beams, and a gap of 1.25 μm between the grillage and the underlying stationary electrode. FEM simulation was used in selecting the flexural spring length to achieve the target design frequency of 250 kHz. The transducer consists of 72 units (a 9 × 8 array) to obtain a target design capacitance, C_0, of 5.8 pF, calculated based upon the net area of the grillage. Figure 3b shows the *C-V* plot, referring to the capacitance as a function of applied DC voltage. A capacitive spring-mass system should show an increase in capacitance with applied DC voltage, because the electrostatic attraction force will deflect the system, reduce the gap, and thereby increase the capacitance. The *C-V* plot confirms the expected behavior of the transducer, but it indicates a C_0 near 10.9 pF. Subsequent FEM simulations show that the capacitance closely approximates that of the gross area of a whole plate rather than the net area of a grillage; in other words, the "cutouts" between grillage beams do not diminish the capacitance. Figure 3c shows the admittance plot in the vicinity of resonance, which is observed to occur near 160 kHz. (The difference between predicted and observed frequency is attributed to support flexibility and to fabrication deviations in the spring width.) Figure 3c depicts the sharpness of resonance, from which a *Q* near 6.7 is extracted. A comparable perforated plate transducer (as depicted in Fig. 1b) with a resonant frequency of 182 kHz displayed a *Q* near 2.0, so the grillage geometry represents substantial improvement. (Considering squeeze-film and radiation damping in air, by theory, *Q* will increase with frequency, and comparisons must be taken between transducers at comparable resonant frequencies.) Compared to a perforated plate, we predicted that the grillage geometry would decrease damping by permitting freer venting of the air beneath the grillage, reducing squeeze- film damping; we interpret these results as evidence qualitatively confirming that prediction.

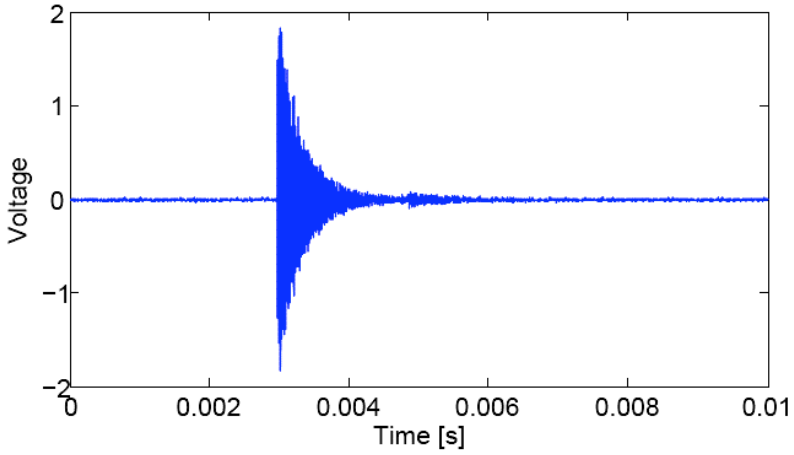

Fig. 4: Pencil lead break response of out-of-plane sensor.

Figure 4 shows the characteristic response of the out-of-plane sensor to a pencil-lead break applied directly to the ceramic package, which is consistent in appearance with the higher *Q* demonstrated by the device.

Finger Transducer for In-Plane Motions

Finally, we report on another new 2007 transducer, designed to sense in-plane motion. It is a finger-type (comb-type) capacitive transducer with a design frequency of 250 kHz. The predicted *Q* is much higher (predicted damping is much lower) than for out-of-plane sensors,

because in-plane motion mostly produces a direct shearing of air in the gap, rather than a squeeze-film or radiation actuation of the air. At the same time, squeeze-film damping in the out-of-plane direction is used beneficially to isolate the desired in-plane mechanical response from the unwanted out-of-plane response.

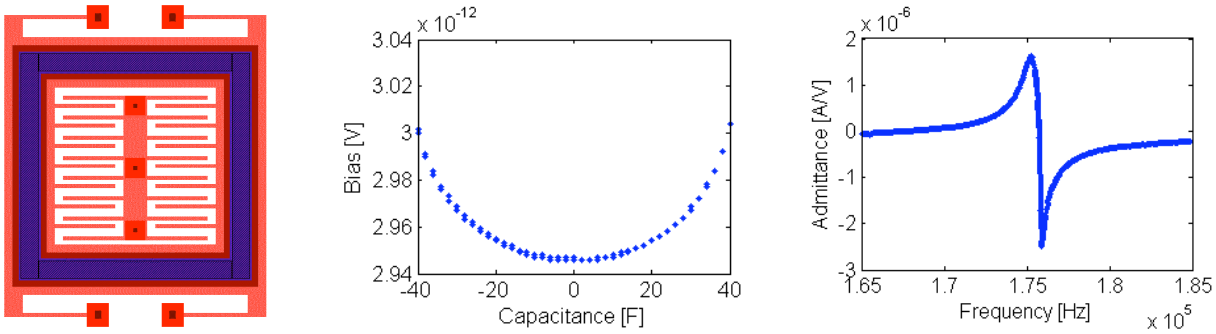

Fig. 5a. CAD layout of finger-type transducer to sense in-plane motion in the y-direction. 5b. *C-V* plot, $C_0 = 2.95$ pF. 5c. Admittance at resonance, $f = 176$ kHz, $Q = 197$.

Figure 5a is the CAD layout of a single unit (128 × 132 μm) showing a stationary central spine with projecting fingers, which form capacitors in relation to fingers that project from a frame supported by four flexural springs and oriented to sense motion in the y-direction; the pitch between fingers is unsymmetrical in order to effect a change in capacitance during motion. Again, FEM simulation was used in selecting the flexural spring length to achieve the target design frequency of 250 kHz, and to calculate the predicted capacitance C_0, which is significantly and beneficially influenced by the effects of fringe capacitance. The transducer consists of 532 units (a 19 × 28 array) to obtain a target design capacitance, C_0, of 3.1 pF. Figure 5b shows the *C-V* plot, confirming the expected behavior of the transducer with a measured C_0 near 2.95 pF. Figure 5c shows the admittance plot in the vicinity of resonance, which is observed to occur near 176 kHz, and the sharp resonance corresponds to a Q near 197. The characterization measurements confirm the design characteristics outlined above, and suggest that the transducer may provide a practical approach to sensing in-plane particle displacements. In principle, the transducer can be fabricated on one MEMS chip together with a similar transducer orthogonal to it, along with a third transducer sensitive to out-of-plane motion, creating a sensor system responding to the three-dimensional components of particle motion.

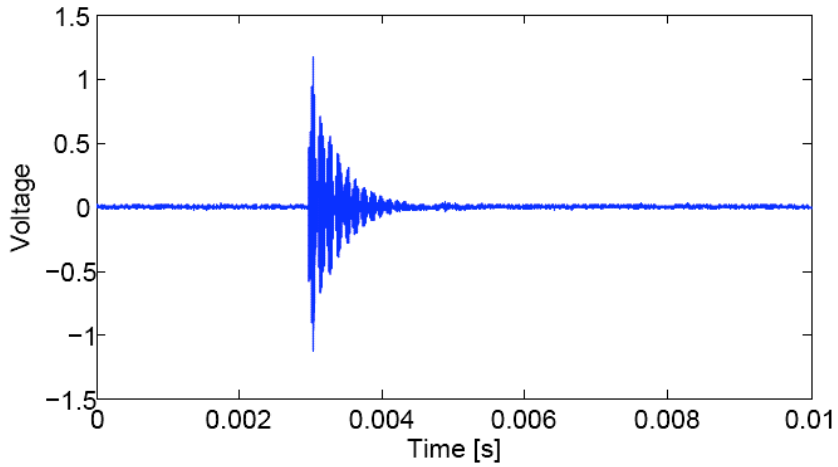

Fig. 6: Pencil-lead break response of in-plane sensor.

Figure 6 shows the response of the in-plane sensor to a pencil-lead break applied directly to the ceramic package. The beat frequency, near 8 kHz, is consistent with a slight difference in frequency between interior and exterior units in the 19×28 sensor array; that frequency difference can be explained by a small difference in their spring lengths, possibly influenced by difference in anchor rigidity. The beat effect is visible only because the in-plane device is a high-Q resonator.

Summary

We have described four recent advances in our understanding of the mechanics of capacitive MEMS transducers resonant in the range between 100 and 500 kHz. We seek to improve the sensitivity of these transducers as acoustic emission sensors, and the advances provide insights for those improvements. Among other factors, damping and noise limit transducer sensitivity, and all four advances guide us to better sensitivity. We have shown an effective laboratory approach for sealing and evacuating a device, thereby reducing the squeeze film and radiation damping effects of air. Characterization experiments show an approximate fourfold increase in quality factor Q, and response of the sensor in pencil lead break testing, after onboard amplification, is compared to the response of a commercial transducer. We have also summarized our recent theoretical analysis of noise, identifying the effective floor to result from Brownian motion and the impact of air molecules with the resonator, confirmed by our measurements. We have reported a significant reduction in squeeze-film damping, in air, when using a grillage of beams as the moving plate rather than a perforated plate with periodically spaced etch holes. Finally, we have reported our first characterization measurements of a new transducer designed to sense in-plane motion. Those results confirm its design characteristics, and show it to be minimally damped (in air) because the in-plane motion mostly produces a shearing of an air volume rather than a squeeze film or radiation excitation of the air volume.

Acknowledgements

This work is supported by the National Science Foundation, Grant CMS-0329880 entitled SENSORS: Collaborative Research: MEMS for Multi-Mode Civil Infrastructure Sensing, and by the Pennsylvania Infrastructure Technology Alliance. We gratefully acknowledge contributions of our research collaborators at Lehigh University, Professor S. P. Pessiki and Dr. D. Ozevin, who is now a Research Scientist with Physical Acoustics Corporation. The opinions, findings, conclusions, and recommendations expressed in this material are those of the current authors and do not necessarily reflect the views of the sponsors or of our collaborators.

References

1. D. Ozevin, D. W. Greve, I. J. Oppenheim, and S. P. Pessiki, Resonant capacitive MEMS acoustic emission transducer, Smart Mater. Struct., **15**, 2006, 1863-1871.

2. D. W. Greve, I. J. Oppenheim, and W. Wu, Modes and Damping in Cmut Transducers for Acoustic Emission, *IEEE Ultrasonics Conf*., 2006.

3. D. W. Greve, I. J. Oppenheim, W. Wu, and A. P. Wright, Development of a MEMS Acoustic Emission Sensor System, *SPIE Smart Structures/NDE Joint Conf*., 2007.

4. B. Bahreyni, C. Shafai, Fabrication of Piezoresistive Sensors in Standard MEMS Foundry Processes, *IEEE Sensors Conf*., 2005.

5. S. D. Senturia, *Microsystem Design*, Springer, 2001, 438.

6. T. B. Gabrielson, Mechanical-thermal noise in micromachined acoustic and vibration sensors, IEEE Trans. Electron. Devices, **40**, 903–909.